ECOLOGY LETTERS

Ecology Letters, (2018) **21**: 1723–1736 doi: 10.1111/ele.13139

REVIEW AND SYNTHESIS

The ecohydrological context of drought and classification of plant responses

Xue Feng,[1]* David D. Ackerly,[2] Todd E. Dawson,[2,3] Stefano Manzoni,[4,5] Rob P. Skelton,[2] Giulia Vico[6] and Sally E. Thompson[7]

Abstract

Many recent studies on drought-induced vegetation mortality have explored how plant functional traits, and classifications of such traits along axes of, for example, isohydry–anisohydry, might contribute to predicting drought survival and recovery. As these studies proliferate, the consistency and predictive value of such classifications need to be carefully examined. Here, we outline the basis for a systematic classification of plant drought responses that accounts for both environmental conditions and functional traits. We use non-dimensional analysis to integrate plant traits and metrics of environmental variation into groups that can be associated with alternative drought stress pathways (hydraulic failure and carbon limitation), and demonstrate that these groupings predict physiological drought outcomes using both synthetic and measured data. In doing so, we aim to untangle some confounding effects of environment and trait variations that undermine current classification schemes, advocate for more careful treatment of the environmental context within which plants experience and respond to drought, and outline a pathway towards a general classification of drought vulnerability.

Keywords

Carbon limitation, classification, hydraulic risk, non-dimensionalisation, plant drought responses.

Ecology Letters (2018) **21**: 1723–1736

INTRODUCTION

Drought mortality and its wider implications

Increasing numbers of drought-associated plant mortality events have been documented worldwide (Allen 2010; Settele *et al*. 2014; Bennett *et al*. 2015). These events are likely to increase in response to global warming, as episodes of low rainfall are exacerbated by rising temperatures (Park Williams *et al*. 2012; Diffenbaugh *et al*. 2015). Large mortality events impact regional water and energy cycles by modifying ecosystem carbon and water balances (Winkler *et al*. 2010; Adams *et al*. 2012) and land atmosphere interactions (Anderegg *et al*. 2013b), and in the most extreme cases may further perturb the global climate system (Phillips *et al*. 2009; Swann *et al*. 2015). Yet, the occurrence of drought mortality remains challenging to predict within existing dynamic global vegetation models (DGVMs), and understanding the ecophysiological drivers of drought mortality remains an area of active research (McDowell *et al*. 2013a; Powell *et al*. 2013; Urli *et al*. 2013; Sevanto *et al*. 2014).

Current uncertainties in models

Partially motivated by the need to reduce uncertainties associated with drought-induced vegetation feedbacks to the climate (Sitch *et al*. 2008; van der Molen *et al*. 2011), DGVMs have started to shift from representing plants through aggregated plant functional types (PFTs) to more flexible trait-based approaches (Van Bodegom *et al*. 2012; Wullschleger *et al*. 2014; Matheny *et al*. 2017). Such efforts would benefit from simplified frameworks that link whole-plant water use – characterised by plant functional traits – to species-level response to drought, an approach suggested in recent syntheses of drought-relevant plant functional traits (Mencuccini *et al*. 2015; Anderegg *et al*. 2016; O'Brien *et al*. 2017). A promising paradigm for characterising species drought responses relates the sensitivity of stomata to water deficit. This paradigm was invoked to explain drought mortality by Cowan (1982), and more recently by McDowell *et al*. (2008) (see also Tardieu *et al*. (1998); McDowell (2011)). It rests on the premise that, because of the basic tradeoff between carbon gain and water loss (Cowan & Farquhar 1977; Cowan 1982), plants with varying degrees of stomatal regulation will be more or less susceptible to carbon limitation or hydraulic failure (i.e. xylem embolism, which limits water transport capacity) under water stressed conditions. While there is a growing consensus that hydraulic failure poses a much greater mortality risk than carbon starvation (Anderegg *et al*. 2015a, 2016; Adams *et al*. 2017; Skelton *et al*. 2017), the precise manner in which these

[1]*Department of Civil, Environmental, and Geo-Engineering, University of Minnesota, Minneapolis, MN, USA*
[2]*Department of Integrative Biology, University of California, Berkeley, CA, USA*
[3]*Department of Environmental Sciences, Policy, and Management, University of California, Berkeley, CA, USA*
[4]*Department of Physical Geography, Stockholm University, Stockholm, Sweden*
[5]*Bolin Centre for Climate Research, Stockholm, Sweden*
[6]*Department of Crop Production Ecology, Swedish University of Agricultural Sciences (SLU), Uppsala, Sweden*
[7]*Department of Civil and Environmental Engineering, University of California, Berkeley, CA, USA*
**Correspondence: E-mail: feng@umn.edu*

carbon and water relations play out during extreme drought, when plants are pushed to their physiological limits, is open to further investigation (O'Brien *et al*. 2014; Rowland *et al*. 2015). Many questions remain over the simultaneous role of biotic interactions (McDowell *et al*. 2011; Anderegg *et al*. 2015b), the buffering capacity of plant water storage (Meinzer *et al*. 2009; Van den Bilcke *et al*. 2013; McCulloh *et al*. 2014), the role of carbon storage products in determining plant water status (Adams *et al*. 2013; Hartmann & Trumbore 2016) and the extent to which xylem refilling may contribute to the reversibility of loss in xylem hydraulic conductance over longer timescales (McCulloh & Meinzer 2015; Trifilo *et al*. 2015). What is clear is that effectively classifying species vulnerability to drought based on measurable plant traits would be useful for evaluating the relative contributions of these ancillary mechanisms and for arriving at simplified trait-based representations of plants within DGVMs.

Developing a classification scheme for drought responses

Existing metrics of drought vulnerability are limited in their ability to predict plant functional outcomes resulting from environmental variations. These metrics are often obtained and reported without considering environmental factors as covariates during experimental design, data collection and data analysis. Yet, because plant responses are influenced by both physiological traits and environmental conditions, the omission of the latter makes it difficult to compare species measured under different environmental conditions, yielding inconsistent rankings across the same set of species (Martínez-Vilalta & Garcia-Forner 2016), and obfuscating the influence of the environment on plant hydraulic strategies (Hochberg *et al*. 2018). We suggest that the time is ripe to critically consider how these metrics relate to the problem of predicting drought mortality across variable environments. In the following sections, we designate a set of criteria as guidelines for constructing a classification scheme for predicting plant drought responses. We stipulate that a set of metrics that forms an effective classification scheme would need to (i) address hydraulic failure and carbon/metabolic limitation as two dominant drought mortality pathways (Hartmann *et al*. 2013; Parolari *et al*. 2014; Mencuccini *et al*. 2015; Rowland *et al*. 2015), (ii) be comprehensive enough to encompass relevant ecophysiological (i.e. trait-based) *and* ecohydrological (i.e. environment based) factors and (iii) effectively separate species within a particular environmental setting along a continuum of drought outcomes.

We proceed by presenting a previously tested model of soil-plant hydraulics that couples plant water status to its ecohydrological environment, and predicts the outcomes of interest (hydraulic failure risk and net carbon assimilation; Feng *et al*. (2017)). The model – tested here with sapflow measurements from a set of Australian species (SI) – accounts for a broad suite of traits and environmental parameters, the importance of which is later explored via sensitivity analysis. To progress towards a classification scheme of plant drought responses, dimensional analysis is used to consolidate model parameters (i.e. traits and environmental conditions) into functionally meaningful groups, which form the basis of the classification system. The efficacy of this set of trait-environment groups is then tested in two cases: first in a set of synthetic plants with traits derived by perturbing the measured traits of *Juniperus monosperma* and *Pinus edulis*, and then across a broader set of species in a desert chaparral biome. We show that the non-dimensional groups can effectively differentiate simulated drought responses both across species within the same site, as well as across intraspecific trait variations. The classification system is yet to be tested against a larger population of plants across different sites, and its predictive ability with respect to drought mortality *in situ* remains to be validated. While acknowledging these limitations, we present our model-based approach as a promising path forward, and outline a roadmap for classifying plants based on their susceptibility to different durations and intensities of drought.

A MODELLING APPROACH TO CLASSIFYING DROUGHT OUTCOMES

Existing classification schemes for plant responses reflect two contrasting approaches to classification (Noble and Gitay, 1996; Symstad, 2002). *A priori* approaches use subjective or deductive reasoning about how a system should operate to define classes or groups (Noble and Gitay, 1996; Bugmann, 1996). For example, the classification of species into groups of a common PFT (the classification approach widely used in DGVMs) reflects an *a priori* assumption that growth forms are correlated with specific trait values, and are thus constrained to certain ranges of realisable primary production and transpiration rates. On the other hand, *a posteriori* approaches formulate groups based on statistical analyses of data sets and identification of major axes of functional variation (Wright *et al*. 2006). Many of the existing drought vulnerability metrics were formulated by examining plant physiological data obtained from experimental manipulations and across environmental gradients.

Both approaches for defining a classification scheme present potential challenges – *a priori* approaches risk subjectivity and bias in our understanding of key controls on plant functional outcomes, while *a posteriori* approaches risk omitting important control variables that have not been included in the data sets. To partially mitigate these challenges, we adopt an alternative approach to classification that begins with a general process-based model that links plant- and site attributes with drought responses. Process-based models have been used previously to identify traits for inclusion in classification schemes, as in the definition of r and K selection strategies (Pianka 1970) based on links to the corresponding parameters in the logistic growth equation (Verhulst 1838), but have not been widely adopted for classifying plant ecophysiology and environmental sensitivity.

The model adopted here for plant drought responses is based on a detailed stomatal response model (Dewar 2002) that is coupled to a plant hydraulics model governed by the hydrodynamic principle of pressure-mediated flow. It simultaneously tracks plant water status and water use and accounts for plant-soil moisture feedback. The particular formulation of the plant hydraulics model was first introduced in Manzoni *et al*. (2014), though its physical premise is based on the well-

established fluid mechanics principle of one dimensional, laminar Hagen-Poiseuille flow (Sutera & Skalak 1993) and has been invoked in similar forms in other plant hydraulics models (Whitehead *et al*. 1984; Sperry *et al*. 1998, 2016; Martínez-Vilalta *et al*. 2002; Daly *et al*. 2004; Sperry & Love 2015). This formulation has previously captured species' differences in hydraulic risks and sensitivities to seasonal rainfall changes (Feng *et al*. 2017). We briefly summarise the model rationale and equations here; for more detailed descriptions, readers are referred to the references above. Model codes are available at https://github.com/feng-ecohydro/soil-plant-model.

Plant hydraulics model

The plant hydraulics model comprises a series of flux-gradient relationships spanning the soil-plant-atmosphere continuum (SPAC). It is applicable at the daily scale, assuming equilibrated, daily-averaged water flux E ($m^3\ day^{-1}$) along the SPAC and negligible water storage within the plant (Fig. 1). Water potentials are interpreted as daytime averages, nighttime fluxes are assumed to be negligible and gravitational effects are neglected. The resistances along the SPAC are modelled as continuous resistances; a matrix flux potential Φ serves to drive the flow and is derived by integrating a hydraulic conductance k across gradients of water potential ψ, that is, $\Phi = \int_{-\infty}^{\psi_i} k(\psi)d\psi$, using the Kirchhoff transform (Ross & Bristow 1990; Sperry *et al*. 1998). Thus, the daily water flux along the soil root interface and within the stem is given by

$$E = -\int_{\psi_X}^{\psi_L} k_X(\psi)d\psi = -(\Phi_L - \Phi_X).$$
$$E = -\int_{\psi_S}^{\psi_X} k_R(\psi)d\psi = -(\Phi_X - \Phi_S), \quad (1)$$

where ψ_S, ψ_X, ψ_L are the water potentials in the soil, stem and leaf (MPa); k_R, k_X are the soil-root and stem conductances ($m^3\ d^{-1}\ MPa^{-1}$), which vary as functions of local water potentials. The tissue level conductances are responsive to local tissue water potential, declining from their maximum values (subscript max) as

$$k_X(\psi_X) = k_{X,max}\left(1 - \frac{1}{1 + e^{a\left(min\left[\psi_X, \psi_{X,min}\right] - \psi_{X50}\right)}}\right) \quad \text{or}$$
$$k_{X,max}e^{-a\,min\left[\psi_X, \psi_{X,min}\right]},$$
$$k_R(\psi_S) = k_{R,max}s^{c-d} = k_{R,max}\left(\frac{\psi_{S,sat}}{\psi_S}\right)^{\frac{c-d}{b}}. \quad (2)$$

Xylem conductivity is modelled as an exponential sigmoidal function (Pammenter & Willigen 1998) or an exponential function (depending on the species), where ψ_{X50} is the water potential at 50% loss relative to maximum xylem conductivity $k_{X,max}$, and a is a fitting parameter. The minimum stem water potential $\psi_{X,min}$ represents the lowest stem water potential that the plant has experienced during a dry down period, and evaluating the stem conductance at $min\left[\psi_X, \psi_{X,min}\right]$ ensures that there is no repair of xylem damage over multiple refilling cycles once conductance has been lost. This assumption is reasonable in climates with a prolonged dry period (e.g. summer drought), during which xylem cannot be readily repaired, and new xylem is not grown. The soil-root conductance k_R declines according to a power law defined by the soil water retention curve, where $\psi_S = \psi_{S,sat}s^{-b}$, $c = 2b + 3$ and $\psi_{S,sat}$ is the water potential near soil saturation and air entry point (Clapp & Hornberger 1978). The parameter $d = 4$ reduces the concavity of the soil hydraulic conductivity-soil moisture relation to account for root extension in drying soil (Daly *et al*. 2004). The maximum conductances ($m^3\ d^{-1}\ MPa^{-1}$) are defined on a per plant basis as

$$k_{X,max} = \frac{k_{sap}T_dA_X}{L_X\rho_w}, \quad (3)$$

$$k_{R,max} = \frac{vK_{S,sat}A_R}{\rho_w g}\sqrt{\frac{RAI}{d_R Z_r}},$$

where k_{sap} is the sapwood area specific hydraulic conductivity of the stem ($kg\ m^{-1}\ s^{-1}\ MPa^{-1}$), A_X is the sapwood area (m^2), L_X is the mean canopy height (m), $K_{S,sat}$ is the saturated soil hydraulic conductivity ($m\ d^{-1}$), A_R is the ground area under which roots are located (m^2), RAI is the root area index ($m^2\ m^{-2}$), Z_R is the mean rooting depth (m), and d_R is the fine root diameter (m). The other coefficients in Equation (3) are unit conversion factors and are listed with all parameters in Table 1.

Plant stomatal response and photosynthesis

The plant hydraulics model (1) presents a set of two equations for three variables: ψ_X, ψ_L and E; to constrain the system further we adopt a model for stomatal conductance based on Dewar (2002). To start, the instantaneous transpiration rate per unit leaf area E' (mol $H_2O\ m^{-2}\ s^{-1}$) is considered as a product of the stomatal conductance g_S (mol air $m^{-2}\ s^{-1}$) and vapour pressure deficit D (mol H_2O/mol air), that is,

$$E' = g_S D = e_d g_{S,C} D, \quad (4)$$

where $g_{S,C} = g_S/e_d$ is the stomatal conductance to air at the leaf level (mol air $m^{-2}\ s^{-1}$), and $e_d = 1.6$ is the ratio of the diffusivities of air and water vapour. The instantaneous transpiration flux is related to the daily transpiration rate E ($m^3\ d^{-1}$) via the tree total leaf area A_C (m^2; assumed to be constant) through $E = E'A_C V_w T_d$, with T_d being the day length in seconds and V_w the molal volume of water ($m^3\ mol^{-1}\ H_2O$). An expression for stomatal conductance $g_{S,C}$ as a function of leaf water potential ψ_L (MPa), vapour pressure deficit D, abscisic acid concentration [ABA] (mol^{-1} ABA m^{-3}), gross photosynthesis A (mol $CO_2\ m^{-2}\ s^{-1}$) and respiration R (mol $CO_2\ m^{-2}\ s^{-1}$) (see equation (7a) of Dewar (2002)) is reduced by constraining it with the maximum stomatal conductance rate based on measured maximum conductance for water vapour, $g_{S,max}$ (mol air $m^{-2}\ s^{-1}$; assuming that it was measured when $D = D_0$ and leaves were well watered), to yield,

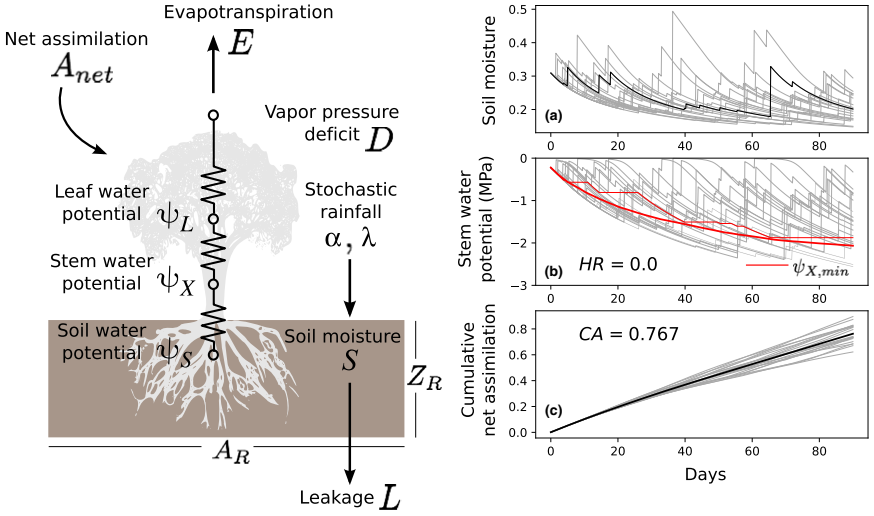

Figure 1 Schematic of the coupled soil-plant hydraulics model (left) with simulated trajectories (right) of (a) soil moisture and (b) stem water potential, and (c) cumulative net assimilation (normalised by maximum) over a dry period. Model parameters use plant traits from *Pinus edulis* (Table S2) and set D = 2.0 kPa, $\lambda = 0.1$ d^{-1}, $\alpha = 0.010$m, and initial soil moisture value $s_0 = 0.31$, in a loamy sand soil ($\psi_{s,sat} = -0.17$ MPa, $b = 4.38$, $K_{S,sat} = 1.0$ m d^{-1}). The thin black line in (a) and the thin red line in (b) correspond to a single trajectory of soil moisture and minimum stem water potential, respectively, and the thick red line corresponds to the minimum stem water potential averaged over 100 trajectories. The solid black line in (c) denotes the ensemble mean of cumulative net assimilation. The values for HR and CA are calculated using the ensemble of trajectories as $CA = 0.767$ and $HR = 0.0$ (i.e. for this scenario, xylem function was never seriously impaired in the simulations).

$$g_{S,C} = \frac{2g_{S,max}}{e_d\left(1+\frac{D}{D_0}\right)} e^{-[\mathrm{ABA}]_r e^{m\psi_L}}. \quad (5)$$

Thus, the stomatal conductance becomes a function of ψ_L, D, and [ABA] only, with r, m, D_0 as sensitivity parameters for [ABA], ψ_L and D respectively (m^3 mol^{-1} ABA; MPa^{-1}; mol air mol^{-1} H_2O). The final piece necessary to close the expression for stomatal conductance is the leaf xylem abscisic acid concentration, which is described by (Dewar 2002)

$$[\mathrm{ABA}] = -\frac{\lambda_{\mathrm{ABA}}\psi_L}{E' + a_s V_w}, \quad (6)$$

where λ_{ABA} is the abscisic acid synthesis rate in the leaf (mol ABA MPa^{-1} m^{-2} s^{-1}) and a_s is the abscisic acid sequestration rate (mol H_2O m^{-2} s^{-1}).

The instantaneous net assimilation A per unit leaf area is described by a diffusion process regulated by stomatal conductance, or,

$$A - R = g_{S,C}(\psi_L)(c_a - c_i), \quad (7)$$

where c_a is the atmospheric CO_2 concentration (mol CO_2 mol^{-1} air). Assuming rapid equilibration of the stomatal cavity, the diffusion process has to match the photosynthetic demand inside the leaf set by:

$$A = kc_i, \quad (8)$$

where k is the carboxylation efficiency (mol air m^{-2} s^{-1}); that is, the slope of the photosynthesis-internal CO_2 concentration relation under CO_2 limitation, which can be related to the kinetic properties of the photosynthetic machinery (e.g. using Farquhar *et al.* (1980) model of photosynthesis). Here, we employ the simplest model of photosynthesis for mathematical convenience, in which light dependency can be incorporated into the kinetic constant k (Hari *et al.* 1986). Combining the previous equations (7) and (8), internal CO_2 concentration c_i can be eliminated, yielding:

$$A - R = \frac{g_{S,C}(kc_a - R)}{k + g_{S,C}} = \frac{g_S(kc_a - R)}{e_d k + g_S}. \quad (9)$$

Thus, the assimilation rate can be directly calculated from the stomatal conductance, the carboxylation efficiency, and the atmospheric CO_2 concentration. We define A_{max} as the maximum measured assimilation rate under well-watered conditions (i.e. when g_S is maximised at $g_{S,max}$), and the leaf respiration rate as a constant proportion of A_{max}, that is, $R = \rho A_{max}$ (Givnish 1988). Neglecting night respiration and all other plant respiration, we define A_{net} as the difference between gross daily assimilation and leaf respiration, or $A_{net} = (A - R)T_d$, where A and R are instantaneous assimilation and leaf respiration rates (mol CO_2 m^{-2} s^{-1}).

Soil-plant feedback and meteorological inputs

To situate the plant within an ecohydrological context, the plant hydraulics model is coupled to a soil moisture balance model that responds to temporal fluctuations in hydrometeorological conditions at the daily scale for a prescribed mean daytime vapour pressure deficit D. The relative soil moisture s over the plant rooting depth Z_R and area A_R (such that $A_R Z_R$ is the volume of soil explored by the roots) is maintained by input through rainfall and outputs from storage-excess runoff and leakage $L = K_{S,sat}s^{2b+3}$ (m^3 day^{-1}), as well as daily plant transpiration E (m^3 day^{-1}) (Porporato *et al.* 2004; Rodriguez-Iturbe & Porporato 2004) (Fig. 1). Rainfall is generated stochastically from a marked Poisson process, with

Table 1 Variables and parameters used for the plant hydraulics and soil water balance model

Symbol	Definition	Units
	Physiological parameters	
A_C	Leaf area	m^2
A_R	Root area; ground area explored by roots	m^2
A_X	Stem cross-sectional area	m^2
L_X	Mean canopy height	m
RAI	Root area index; ratio of root areal coverage per ground area	$m^2\ m^{-2}$
$g_S, g_{S,max}$	Leaf scale stomatal conductance of H_2O	mol air $m^{-2}\ s^{-1}$
k_{sap}	Sapwood area specific hydraulic conductance	kg $m^{-1}\ s^{-1}\ MPa^{-1}$
a	Exponent on the xylem vulnerability curve	–
ψ_{X50}	Xylem water potential corresponding to 50% loss in stem conductance	MPa
$\psi_{X,min}$	Minimum xylem water potential experienced to date	MPa
ψ_{g12}	Leaf water potential corresponding to stomata closure, $\psi_{g12} = \log(0.12)/m$	MPa
d_R	Fine root diameter	m
Z_R	Mean rooting depth	m
A, A_{max}	Instantaneous gross assimilation rate	mol $CO_2\ m^{-2}\ s^{-1}$
R	Instantaneous leaf respiration rate	mol $CO_2\ m^{-2}\ s^{-1}$
A_{net}	Daily net assimilation rate ($= (A - R)T_d$)	mol $CO_2\ m^{-2}\ d^{-1}$
k	Carboxylation capacity	mol air $m^{-2}\ s^{-1}$
c_i, c_a	Internal leaf and ambient CO_2 concentration	mol $CO_2\ mol^{-1}$ air
λ_{ABA}	ABA synthesis constant in the xylem	mol ABA $MPa^{-1}\ m^{-2}\ s^{-1}$
D_0	Stomatal sensitivity to vapour pressure deficit	mol $H_2O\ mol^{-1}$ air
m	Stomatal sensitivity to leaf water potential	MPa^{-1}
r	Stomatal sensitivity to ABA concentration	$m^3\ mol^{-1}$ ABA
	Upscaled tree-level parameters	
$k_X, k_{X,max}$	Stem scale xylem conductance	$m^3\ d^{-1}\ MPa^{-1}$
$k_R, k_{R,max}$	Bulk soil-root hydraulic conductance	$m^3\ d^{-1}\ MPa^{-1}$
Λ_{ABA}	ABA synthesis rate in the xylem	mol ABA $MPa^{-1}\ d^{-1}$
K	Carboxylation capacity at canopy level	mol air d^{-1}
$g_{C,max}$	Maximum canopy conductance	m^3 mol air d^{-1} H_2O
R_C	Respiration rate	mol $CO_2\ d^{-1}$
	Ecohydrological parameters	
α	Mean rainfall depth	m
λ	Mean rainfall frequency	d^{-1}
D	Vapour pressure deficit averaged over daytime	mol $H_2O\ mol^{-1}$ air
s_0	Initial soil moisture value at the beginning of dry period	–
t_{dry}	Dry period	d
n	Soil porosity	–
b	Exponent of the soil water retention curve (Clapp & Hornberger 1978)	–
$\psi_{S,sat}$	Water potential near soil saturation (Clapp & Hornberger 1978)	MPa
$K_{S,sat}$	Saturated soil hydraulic conductivity	m d^{-1}
	Model variables	
s	Relative oil moisture averaged over rooting depth	–
ψ_S	Soil water potential	MPa
ψ_X, ψ_L	Water potential in the xylem and leaf	MPa
E	Transpiration rate	$m^3\ d^{-1}$
[ABA]	ABA concentration in the leaf	mol ABA m^{-3}
$g_{S,C}$	Stomatal conductance at the leaf level	mol air $m^{-2}\ s^{-1}$
	Other constants	
c	Exponent of the soil hydraulic conductivity curve, $c = 2b + d$	–
d	Exponent of the root growth correction factor, $d = 4$	–
e_d	Ratio of the diffusivities of air and water vapour, $e_d = 1.6$	–
g	Gravitational acceleration, $g = 9.81$	$m\ s^{-2}$
T_d	Day length in seconds, $T_d = 36\ 000$	s d^{-1}
ρ_w	Density of water, $\rho_w = 1000$	kg m^{-3}
V_w	Molal volume of water, $V_w = 18 \times 10^{-6}$	$m^3\ mol^{-1}$ H_2O
ν	Conversion factor, $\nu = 10^6$	Pa MPa^{-1}

mean daily frequency λ (day^{-1}) and mean event size α (m) per unit ground area. Plant transpiration E provides the key link to plant water use as defined by plant functional traits, as it responds to vapour pressure deficit D and soil water potential ψ_S, which is in turn linked to s through the soil water retention curve $\psi_S = \psi_{S,sat} s^{-b}$ (Clapp & Hornberger 1978). The time course of plant water use is dynamically linked to soil moisture through the amount of water left in the soil over the course of a season and the sensitivity of plant water uptake rates to this soil water availability. To more accurately represent plant responses over multiple rewetting cycles during the dry period, the minimum stem water potential $\psi_{X,min}$ – the lowest stem water potential the plant has ever experienced at time t – is updated at each time step so that it can be used to evaluate a stem conductance, assuming no xylem refilling.

With the set of five equations in (1), (4), (5), and (6), ψ_X, ψ_L, E, $g_{S,C}$ and [ABA] can be solved simultaneously once environmental conditions such as soil type, soil water potential ψ_S and vapour pressure deficit D, as well as the minimum stem water potential $\psi_{X,min}$ (updated whenever $\psi_X < \psi_{X,min}$), are known. The resulting stomatal conductance $g_{S,C}$ can then be used to calculate net assimilation A_{net} based on the assimilation rate A from equation (9). To assess if this hydraulic model provides reasonable predictions over a single dry season – which then allows extrapolating results to ensembles of rainfall realisations – the model was validated against sapflow data for three Australian species, as described in the SI (with normalised root mean square errors of 0.158, 0.138 and 0.167).

Indices of drought outcomes

Two indices of plant performance are defined: seasonal hydraulic risk HR (unitless) and normalised seasonal net carbon assimilation CA (unitless). They are derived from the simulated trajectories of minimum stem water potential $\psi_{X,min}$ and net assimilation A_{net} over a dry period t_{dry} (the exact paths of these trajectories will differ due to different realisations of rainfall events (Fig. 1)). We focus on dry periods of

the year when water stress is likely (which are clearly identifiable in seasonally dry climates, but can also be found more broadly). Seasonal hydraulic risk HR is defined as the expected proportion of time over t_{dry} during which $\psi_{X,min}$ (thin red line, Fig. 1b) lies below a critical threshold, over all realisations of $\psi_{X,min}$. Here, the threshold is designated by the xylem potential corresponding to a 50% loss in stem conductivity, ψ_{X50}. The normalised seasonal net carbon assimilation CA is defined as the ensemble mean of the cumulative net assimilation at the end of the dry season, divided by the maximum net assimilation over this period $(A_{max} - R)T_d t_{dry}$. As plants can cease carbon uptake while still undergoing respiration, it is theoretically possible for them to have negative CA after long dry periods. In this case, their carbon balance during the dry period is negative, indicating a depletion of non-structural carbohydrates. The high correlation between modelled seasonal hydraulic risk HR and a measured proxy of stem hydraulic safety – the difference between the lowest xylem water potential observed during the dry season and ψ_{X50}, or $\psi_{X,min}$ – for a set of desert chaparral species (Fig. S5) and the theoretical relation between CA and carbohydrate dynamics (SI) give us confidence that the model is able to make realistic predictions of drought outcomes.

SENSITIVITY ANALYSIS OF DROUGHT OUTCOMES

Explicitly defining drought outcomes allows us to quantify their dependence on ecophysiological and ecohydrological variables. Here, we carry out a Sobol' global sensitivity analysis (Sobol' 2001) to identify the most important plant functional traits and environmental variables for determining seasonal hydraulic risk (HR) and normalised seasonal carbon assimilation (CA). This type of information can be used to (i) reduce prediction uncertainty using data to constrain the influence of various parameters, (ii) judiciously allocate resources to acquire such data in the field and (iii) reduce the complexity of the problem by treating parameters that have little influence on the predictions as constants. The total order indices from a Sobol' sensitivity analysis measure the contribution of the variance in each parameter to the variance of the output, including the effects of interactions with all other model parameters. A higher order index suggests a stronger dependence of the outcome on the specified input variable.

Though sensitivity analysis can be generally applied to a model using any reasonable range of parameter values, we define our parameter ranges based on observed trait and environmental data to account for the effects of trait covariation across species. Data from co-occurring species in two settings were used: (i) *Juniperus monosperma* and *Pinus edulis* (McDowell *et al.* 2008), and (ii) a set of desert chaparral species in Southern California (Pivovaroff *et al.* 2016). Though methods for obtaining xylem vulnerability measurements are increasing under review within the plant physiology community (Skelton *et al.* 2018), the conclusions from the sensitivity analysis should not hinge on the precise observed values. To perform the sensitivity analysis, each of the input parameters was varied randomly from 0.5 to 2 times the observed value for a given species. While the intraspecific variability in some hydraulic traits is relatively small (e.g. ψ_{X50}, TRY dataset 'Plant Hydraulic Traits' (ID: 197) (Kattge *et al.* 2011)), and other traits may exhibit greater degrees of intraspecific variation (Anderegg 2015; Siefert *et al.* 2015), this four-fold range was consistently applied to all trait and environmental parameters. Measured maximum daily assimilation rates were used to infer the carboxylation capacity k (mol air m^{-2} d^{-1}) under well-watered conditions, using equation (9) with measured values of $g_S = g_{S,max}$. Parameter values in both settings are listed in Tables S2 and S3.

Results show that seasonal hydraulic risk and normalised seasonal carbon assimilation are differentially responsive to plant ecophysiological traits (Fig. 2). Seasonal hydraulic risk is most sensitive to xylem vulnerability (ψ_{X50}) and stomatal response to leaf water potential (m) for all species. On the other hand, seasonal carbon assimilation is generally most sensitive to morphological traits like canopy and rooting area and rooting depths (A_c, A_R, and Z_R) as well as maximum daily assimilation rate (A_{max}), followed by environmental variables like vapour pressure deficit (D) and rainfall frequency (λ, for *Juniperus monosperma* and *Pinus edulis*) or length of the growing season (t_{max}, for chaparral species). Evidently, while hydraulic risk is more sensitive to parameters that regulate the *rates* of physiological response to the progression of drought (e.g. stomatal closure, xylem vulnerability), seasonally integrated carbon assimilation is more sensitive to parameters that determine the overall *capacity* of water supply and demand (e.g. canopy and rooting size, rainfall rates and evaporative demand). The degrees to which hydraulic risk and carbon assimilation are sensitive to different sets of parameters suggest that they should be considered as independent outcomes for the sake of model calibration and testing, and are interacting and simultaneous, rather than dichotomous, pathways to mortality (McDowell *et al.* 2013b; Mencuccini *et al.* 2015).

Another notable result is that, within the same community, species outcomes also tend to be more sensitive to certain *clusters* of parameters. This is especially evident in the relative rankings of parameter sensitivities across the desert chaparral species. For example, within the desert chaparral community, species whose hydraulic risks are most sensitive to variations in xylem vulnerability (ψ_{X50}) are also most sensitive to stomatal response to leaf water potential (m). On the other hand, the species whose hydraulic risks are most sensitive to canopy and rooting area (A_c and A_R) are also most sensitive to maximum stomatal conductance ($g_{S,max}$). Likewise, for seasonal net assimilation, those that are more sensitive to rooting depth (Z_R) are also less sensitive to vapour pressure deficit (D), suggesting that increased soil water storage can compensate for variations in atmospheric demand. These trait clustering suggests potential tradeoffs and co-variations among functional traits (Bartlett *et al.* 2016, Martin-StPaul *et al.* 2017) and environmental conditions that contribute to drought outcomes. Resolving these potential co-variations within the model may help elucidate the specific pathways through which plants die from drought (Mencuccini *et al.* 2015).

DIMENSIONAL ANALYSIS PRODUCES INDEPENDENT AXES FOR DROUGHT RESPONSE CLASSIFICATION

To further examine the relationships between trait parameters, we apply dimensional analysis to consolidate a set of model

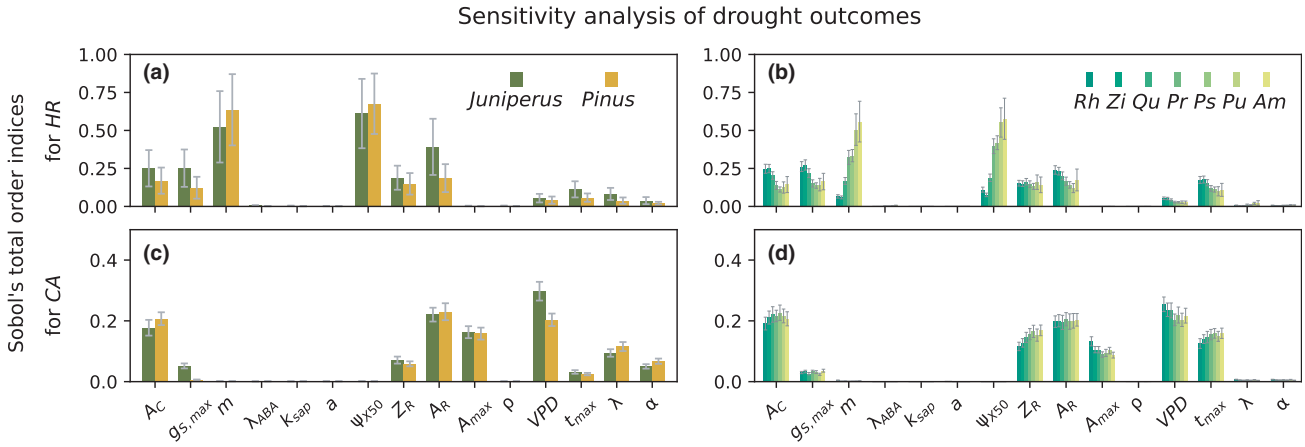

Figure 2 Sensitivity analysis of seasonal hydraulic risk, *HR* (a and c), and normalised seasonal carbon assimilation, *CA* (b and d), to various plant traits and environmental parameters, shown for co-occurring species in two settings: *Juniperus monosperma* and *Pinus edulis* (a and b), and a set of desert chaparral species (c and d). Environmental parameters were set to $D = 2.0$ kPa, $t_{dry} = 180$ days, $\lambda = 0.1$ d^{-1} and $\alpha = 10$ mm for panels a-b, and $D = 2.0$ kPa, $t_{dry} = 240$ days, $\lambda = 0.05$ d^{-1} and $\alpha = 1.7$ mm for panels c-d, based on field conditions. Soil parameters for both are $\psi_{s,sat} = -0.17 \times 10^{-3}$ MPa, $b = 4.38$, $K_{S,sat} = 1.0$ m d^{-1} and $s_0 = 0.31$. To perform the sensitivity analysis, all trait and environmental parameters were varied from 0.5 to 2 times their observed value. Whiskers correspond to 95% confidence intervals for the total order indices. The desert chaparral species are abbreviated as the following: Rh, *Rhus ovata*; Pu, *Purshia tridentata*; Qu, *Quercus cornelius-mulleri*; Am, *Ambrosia salsola*; Ps, *Psorothamnus arborea*; Pr, *Prunus fasciculatum*; Zi, *Ziziphus parryi*.

parameters into a reduced set of non-dimensional groups that determine the system behaviour. Dimensional analysis is a formalised procedure in physics and engineering applications for simplifying high dimensional problems and obtaining insights into relationships between physical quantities (Strogatz 1994; Barenblatt 1996). The Reynolds number from fluid mechanics is perhaps the best-known example of a dimensionless group. It is used to classify fluid flow as laminar, turbulent or transitional and is applicable and interpreted in the same way independently of variations in fluid density, velocity, viscosity and setting (e.g. in stream channels or pipe cross sections). The non-dimensional groups that are generated from dimensional analysis are parameter combinations whose units cancel out. They represent the most parsimonious set of attributes that can be used to describe model predictions. The process of formulating these non-dimensional groups from known functional relationships starts with the selection of a set of dimensionally independent parameters that represents a set of fundamental dimensions. These are then used to reduce all other parameters into dimensionless ratios that will allow us to identify a basic set of classification axes.

To proceed, the coupled hydraulic model can be summarised by noting that the outcomes of interest (seasonal hydraulic risk *HR* and normalised seasonal carbon assimilation *CA*) are functions of a finite set of parameters, consisting of the most influential parameters from the sensitivity analysis as well as other parameters from the plant hydraulics model:

$$\begin{aligned} HR &= f_1\left(\psi_{g12}, g_{S,max}, A_C, k_{sap}, A_X, \psi_{X50}, K_{s,sat}, A_R, Z_R, \psi_{S,sat}, \right. \\ &\quad \left. \lambda_{ABA}, r, D, n, \alpha, \lambda, t_{dry}\right), \\ CA &= f_2\left(\psi_{g12}, g_{S,max}, A_C, k_{sap}, A_X, \psi_{X50}, K_{s,sat}, A_R, Z_R, \psi_{S,sat}, \right. \\ &\quad \left. \lambda_{ABA}, r, D, n, \alpha, \lambda, t_{dry}, k, c_a, R\right), \end{aligned} \tag{10}$$

where n is the soil porosity, which depends on the soil type, and ψ_{g12} is the stomatal closure point, a metric of stomatal sensitivity that is related to m through $\psi_{g12} = \log 0.12/m$. These relationships can be simplified by combining the physiological variables to formulate equivalent conductances and fluxes at the whole-tree level: maximum daily stem and root conductances, $k_{X,max}$ and $k_{R,max}$, according to Equation (3) (subsuming A_X and A_R as well as k_{sap} and $K_{s,sat}$), maximum daily canopy-level conductance $g_{C,max} = g_{S,max} A_C V_w T_d$ (m^3 mol air d^{-1} mol^{-1} H_2O), canopy-level daily carboxylation capacity $K = kA_C T_d$ (mol air d^{-1}), canopy-level daily respiration flux $R_C = RA_C$ (mol CO_2 d^{-1}) and stem-level daily ABA production rate $\Lambda_{\mathrm{ABA}} = \lambda_{ABA} A_X T_d$ (mol ABA MPa^{-1} d^{-1}). We also combine the environmental variables to form the mean daily rainfall rate over the plant ($\bar{P} = \alpha \lambda A_R$; m^3 d^{-1}), and soil water storage accessible by the plant ($W = nZ_R A_R$; m^3). As a result, *HR* and *CA* can be recast as

$$\begin{aligned} HR &= f_1'\left(\psi_{g12}, \psi_{X50}, \psi_{S,sat}, g_{C,max}, k_{X,max}, k_{R,max}, \lambda_{ABA}, \right. \\ &\quad \left. r, D, W, \bar{P}, t_{dry}\right) \\ CA &= f_2'\left(\psi_{g12}, \psi_{X50}, \psi_{S,sat}, g_{C,max}, k_{X,max}, k_{R,max}, \lambda_{ABA}, \right. \\ &\quad \left. r, D, W, \bar{P}, t_{dry}, K, c_a, R_C\right). \end{aligned} \tag{11}$$

Written this way, the model depends on 15 dimensional parameters (*HR* and *CA* are dimensionless) and six primary dimensions – length (e.g. m), time (e.g. second), mass of water vapour (e.g. mol), mass of carbon (e.g. mol), mass of air (e.g. mol) and mass of ABA (e.g. mol). The Buckingham Pi Theorem (Buckingham 1914; Curtis *et al.* 1982; Barenblatt 1996) dictates that the system can be reduced to $15 - 6 = 9$ independent dimensionless parameters (excluding *HR* and *CA*) that consist of ratios of the original dimensional parameters, the so-called Pi groups. This is done by selecting a subset of the parameters that independently encapsulate each of the primary dimensions (Buckingham 1914). By rearranging ratios of Pi groups to form new ones, the non-dimensionalised model can be summarised as (see SI Section 3 for more details):

$$HR = F_1(\beta, \delta, \chi, \kappa, \varepsilon, \tau, \eta),$$
$$CA = F_2(\beta, \delta, \chi, \kappa, \varepsilon, \tau, \eta, \theta, \omega), \quad (12)$$

where the nine dimensionless parameters are $\beta = \frac{\psi_{X50}}{\psi_{g12}}$, $\delta = \frac{\psi_{X50}}{\psi_{S,sat}}$, $\kappa = \frac{k_{X,max}}{k_{R,max}}$, $\chi = \frac{k_{X,max}\psi_{X50}}{g_{C,max}D}$, $\varepsilon = \frac{g_{C,\max}D}{\bar{P}}$, $\tau = \frac{t_{dry}\bar{P}}{W}$, $\eta = \frac{\lambda_{\mathrm{ABA}}r}{k_{X,max}}$, $\theta = \frac{R_C}{Kc_a}$, and $\omega = \frac{KV_w}{g_{C,max}}$. The functions F_1 and F_2 do not have explicit forms due to nonlinearities embedded in the soil-plant system.

The non-dimensional groups of traits in equation (12) that follow from (10) are not unique, but form a comprehensive set of plant- and site-related attributes of drought susceptibility. We describe these groups below; the descriptions given in parentheses correspond to lower and higher values of each group:

(1) ***Hydraulic risk aversion*** $\beta = \psi_{X50}/\psi_{g12}$ (risk-seeking to risk-averse): this group of traits closely resembles the isohydricity metric introduced by Skelton *et al*. (2015) and relates the water potential threshold representative of substantial xylem dysfunction, ψ_{X50}, to that of stomatal closure, ψ_{g12}. High β can arise from more sensitive stomata (more positive ψ_{g12}) and/or reduced xylem vulnerability (more negative ψ_{X50}).

(2) ***Site suitability*** $\delta = \psi_{X50}/\psi_{S,sat}$ (unfavourable to favourable): this group relates the water potential threshold for stem functional integrity ψ_{X50} to the water potential near soil saturation $\psi_{S,sat}$. Typically, loamy and clayey soils with smaller soil pores have more negative $\psi_{S,sat}$ compared to sandy soils (Laio *et al*. 2001; Rodriguez-Iturbe & Porporato 2004), so a high δ for a fixed ψ_{X50} would indicate that a plant is situated on soils that are easier to drain. In such cases, plants can extract water more easily, but the ease of deep drainage also reduces water storage throughout the dry season.

(3) ***Stem transport capacity*** $\kappa = k_{X,max}/k_{R,max}$ (modest to prolific): this group relates maximum conductances in the stem $k_{X,max}$ to that in the root $k_{R,max}$. Higher κ would represent an increased capacity for the stems to transport water from root to shoot. Lower κ would point to a bottleneck within stem transport.

(4) ***Structural demand*** $\chi = k_{X,max}\psi_{X50}/\left(g_{C,max}D\right)$ (sensitive to robust): this group compares a characteristic water flux through the stem to the maximum evaporative flux allowed by stomatal conductance, defined by the product of maximum canopy conductance and vapour pressure deficit. Lower χ would imply an increased atmospheric demand relative to xylem water flux, requiring a larger water potential gradient across the stem to meet the pull of canopy demand.

(5) ***Drought intensity*** $\varepsilon = g_{C,\max}D/\bar{P}$ (mild to intense): this group is a ratio of maximum daily atmospheric water demand – based on the product of vapour pressure deficit and maximum canopy conductance – and mean daily rainfall input. It is in a form analogous to the dryness index (also known as the aridity index) introduced by Budyko (Budyko 1974; Porporato *et al*. 2004; Feng *et al*. 2012) to describe the long-term soil water balance under a variety of climates, except that here the maximum evapotranspiration rate is assumed to be constrained by canopy conductance rather than potential evapotranspiration.

(6) ***Drought duration*** $\tau = t_{dry}\frac{\bar{P}}{W}$ (short to long): This group compares the dry period t_{dry} against a timescale of soil water recharge, calculated as the time to fully saturate a storage $W = nZ_RA_R$ with an average rainfall rate $\bar{P}$. Low mean rainfall rates can increase effective drought duration.

(7) ***Respired fraction*** $\theta = R_C/(Kc_a)$ (low to high rates of respiration relative to photosynthesis): this group relates the ratio of daily respiration to maximum gross photosynthesis without any stomatal limitation (i.e. as stomatal conductance g_C approaches infinity in equation (9)). The respired fraction can decrease due to increases in the atmospheric CO_2 concentration.

(8) ***Water use efficiency*** $\omega = KV_w/g_{C,max}$ (inefficient to efficient in modulating the tradeoff between carbon fixation and water loss during photosynthesis): this group describes the maximum carbon fixation rate per unit of water lost through transpiration under non-water limiting conditions (V_w is the molal volume of water). It is an idealised limit of the intrinsic water use efficiency $A/g_{S,C}$. It can also be related to the ratio of internal to atmospheric CO_2 concentrations by combining equations (7) and (8): $\omega = \frac{c_a}{e_d c_i}\left(1 - \frac{c_i}{c_a}\right)$, where e_d, the ratio of air and water vapour diffusivity, is 1.6.

(9) ***Foliar ABA concentration*** $\eta = \Lambda_{\mathrm{ABA}}r/k_{X,max}$ (less to more foliar concentration of ABA): this group relates ABA production rate in the stem to the maximised stem level hydraulic conductivity. A higher value would suggest a higher concentration of ABA in the leaf xylem.

While most of these non-dimensional groups consist of plant and soil-related hydraulic parameters (two ratios of water potentials and two ratios of hydraulic conductances), some also incorporate soil and atmospheric attributes that characterise features of a drought (intensity ε and duration τ), while others relate to plant metabolic rates (θ, ω, and η). Here, we have used dimensional arguments to propose exact formulations of these groups. Each one represents some attribute of plants and their environment that is needed to fully describe drought outcomes in terms of *HR* and *CA*. The sensitivity analysis previously presented has already suggested that *HR* and *CA* may be more strongly influenced by some of these parameters than others. We proceed by testing the ability of these non-dimensional groups to predict drought outcomes in terms of *HR* and *CA*.

TESTING THE CLASSIFICATION AXES ON DIVERSE PLANT GROUPS

To more closely examine how these emergent relationships among trait and environmental parameters affect drought outcomes, we simulate drought outcomes using measured parameter values. The goal here is not to test model predictions *per se*, but to explore the extent to which the non-dimensional groups can be used to classify strategies of plant water use. In each of the following cases, the model was first parameterised using measured traits, then used to simulate trajectories of $\psi_{X,min}$ and A_{net} in a loamy sand soil, over constant vapour pressure deficit, and subject to stochastic rainfall forcing over a dry period of length t_{dry}. *HR* and *CA* calculated from the seasonal trajectories are then related to the non-dimensional groups.

First, a set of synthetic plant trait combinations for *Juniperus monosperma* is generated to explore a whole morphospace centred on measured trait values (Table S2). Each trait parameter was randomly sampled from a uniform distribution whose range varied from 0.5 to 2 times its measured value,

and each trait combination of the resulting 17 000 randomised parameter sets constitutes a point. In nature, the range of parameter values will likely be larger for some traits than others; in the absence of additional data, we chose this fixed range to maintain consistency across all traits. The modelled drought outcomes and non-dimensional groups for the synthetic plants are shown in Fig. 3.

The results indicate that the proposed non-dimensional groups are capable of distinguishing individual trait variations that result in varying drought outcomes. *HR* was most strongly and negatively correlated with hydraulic risk aversion (β) and site suitability (δ), and positively correlated with structural demand (χ) and drought intensity (ε). Hydraulic risk aversion (β) has negligible influence on *CA*, which instead most strongly and negatively correlated with drought intensity (ε), drought duration (τ) and water use efficiency (ω). Overall, an intense drought due to high daily potential transpiration or low rainfall, or a long drought, will be most likely among all other non-dimensional groups to decrease normalised carbon assimilation *CA* while increasing hydraulic risk *HR*. It is also notable that the relationship between *CA* and ω has a lower bound that increases (likely due to a more efficient use of available water) and an upper bound that decreases, which could result from an increase in $g_{C,max}$ due to more aggressive plant water use that quickly exhausts available soil water. Results for *Pinus edulis* are similar and are shown in Fig. S4.

The second case uses measurements from the set of co-occurring chaparral species in Fig. 2c,d (Pivovaroff *et al.* 2016), which share common soil, site and atmospheric conditions (see model parameter values in Table S3). Because respiration and ABA synthesis rates were not explicitly measured, we omit comparison to the respired fraction θ and ABA sensitivity η. We examined each of the remaining dimensionless groups against simulated *HR* and *CA* from the hydraulics model, parameterised by measured traits for each species, and plotted those that were most strongly correlated with *HR* and *CA*.

Figure 4 shows the relationships between the selected dimensionless groups (based on measured values) and modelled metrics *HR* and *CA* for each species, along with their Spearman rank correlation coefficients. The strongest correlations emerged between the species' seasonal hydraulic risk *HR* and their hydraulic risk aversion β and structural demand χ. This is consistent with results from the sensitivity analysis (Fig. 2c,d), as the variations in the sensitivities to ψ_{X50} and m, which make up the components for β, were the highest among the chaparral species. In addition, having a larger structural demand χ due to higher canopy transpiration would conceivably increase the strain on the hydraulic architecture, thereby increasing a species' hydraulic risk. On the other hand, cumulative carbon assimilation *CA* is strongly correlated with drought intensity ε, with increasing drought intensity drastically decreasing the species' carbon assimilation. The rankings for *HR* and *CA* vary for different species; some, like *Prunus fasciculatum*, can maintain moderately high carbon assimilation despite positive hydraulic risk, while others, like *Juniperus californica,* exhibit exceedingly high carbon assimilation with no hydraulic risk. This suggests a range in the degree to which each co-occurring species may be adapted to drought in its environment, with some like *Juniperus californica* better adapted than others. Comparing these species using non-dimensional groups thus offers a practical way of classifying them according to drought vulnerability.

DISCUSSION

A classification scheme for plant drought vulnerability

The number of potentially relevant traits for drought vulnerability in different biomes (O'Brien *et al.* 2017) gives rise to the

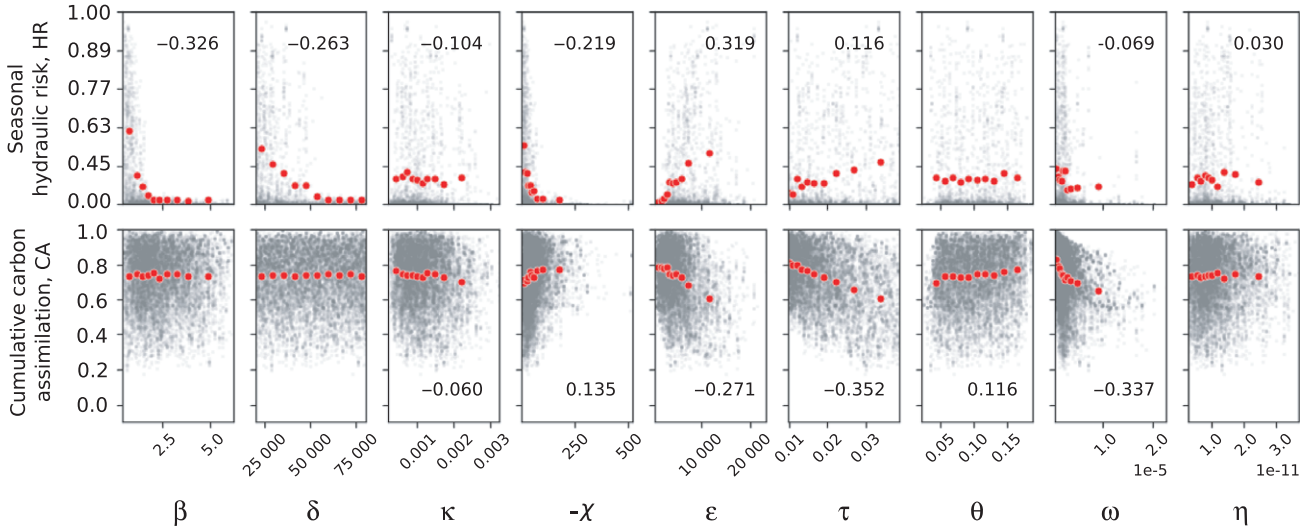

Figure 3 Modeled seasonal hydraulic risk (*HR*) and normalised seasonal net carbon assimilation (*CA*) based on variations in the traits of *Juniperus monosperma*, plotted against nine non-dimensional groups. Grey dots represent individual realisations using randomly selected trait combinations, and the red dots represent their binned averages. Spearman's rank correlation coefficients whose associated *P*-values are less than 0.01 are shown in each plot. Soil and climatic parameters are as follows: $D = 2.0$ kPa, $t_{dry} = 180$ days, $\lambda = 0.1$ d^{-1} and $\alpha = 10$ mm, $n = 0.42$, $\psi_{s,sat} = -0.17 \times 10^{-3}$ MPa, $b = 4.38$, $K_{S,sat} = 1.0$ m d^{-1} and $s_0 = 0.31$. The *x*-axis for structural demand χ is inverted to avoid negative numbers, and the *y*-axis for the *HR* plots have been rescaled by applying the square root function over 0 to 1 to more clearly see vertical trends.

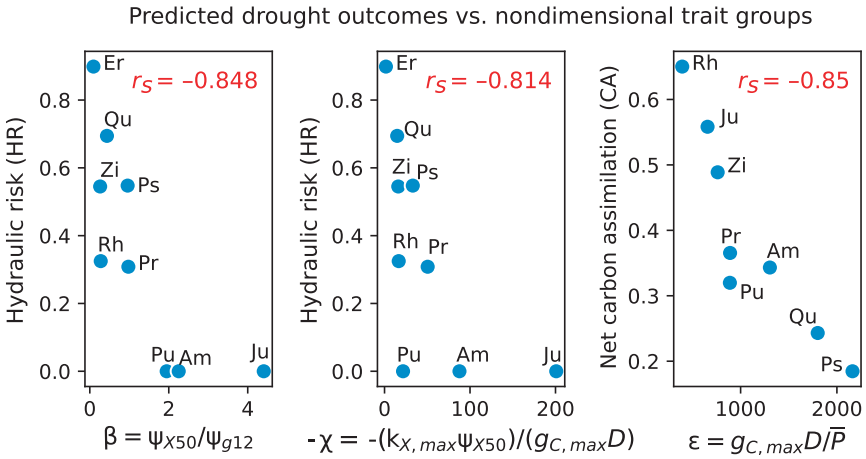

Figure 4 Relationship between modelled mean seasonal hydraulic risk (*HR*) and mean normalised seasonal net carbon assimilation (*CA*) parameterized with measured chaparral species data (Pivovaroff *et al.* 2016). plotted against the most impactful non-dimensional groups: (left) hydraulic risk aversion, (center) structural demand, and (right) drought intensity. Spearman's rank correlation coefficients (r_s) for each set of relationships are shown in red. The species are abbreviated as the following: Rh, *Rhus ovata*; Pu, *Purshia tridentata*; Qu, *Quercus cornelius-mulleri*; Am, *Ambrosia salsola*; Ps, *Psorothamnus arborea*; Ju, *Juniperus californica*; Pr, *Prunus fasciculatum*; Er, *Eriogonum fasciculatum*; Zi, *Ziziphus parryi*. The axis for structual demand χ is inverted to avoid negative numbers.

practical problem of extracting general insights from a high dimensional space. Classification at its core is a process of dimensional reduction, capturing the essential features of a system through a carefully chosen set of variables. This is one of the first steps towards developing an objective classification scheme for plant drought vulnerability (Fig. 5).

Dimensional analysis offers a systematic way to reduce the complexity of the problem (Fig. 5, step 2). It not only formulates independent axes of variation (via dimensionless trait groups) that define a particular drought outcome, but also suggests tradeoffs between traits. For example, while ψ_{X50} and ψ_{g12} have both been identified as strong determinants of hydraulic risk (see also Skelton *et al.* (2015)), dimensional analysis tells us that the effect on hydraulic risk of scaling ψ_{X50} by a factor x should be the same as scaling ψ_{g12} by $1/x$. This establishes the nature of the tradeoff between ψ_{X50} and ψ_{g12}. These axes of variation that form the basis of the classification scheme are summarised in section Dimensional analysis produces independent axes for drought response classification. Many analogues of these non-dimensional groups have been used in previous studies of drought outcomes. For example, drought intensity and duration are often invoked to explain differences in species water use patterns (e.g. Mitchell *et al.* 2013), though an unambiguous, quantitative definition of drought 'intensity' and 'duration' remains elusive. Some of the non-dimensional groups have also emerged in analytical solutions of a minimalist SPAC model (Manzoni *et al.* 2014) and a stochastic soil moisture balance model (Porporato *et al.* 2004; Feng *et al.* 2012). Here, we have explicitly defined drought outcomes (seasonal hydraulic risk and normalised seasonal carbon assimilation) based on a plant hydraulics model to allow for comparison across species, and demonstrated the ability of the dimensionless groups to separate co-occurring species as well as synthetic phenotypes of the same species along the continuum of hydraulic risk and carbon assimilation. When combined with sensitivity analysis, this provides insights into how the overall problem can be made more parsimonious by suggesting tradeoffs between parameters and identifying those with little to no impact on the drought outcomes.

Broadening the drought response classification to include ecohydrological variables

We also contend that an effective drought classification system would fulfil three criteria: it would be (i) oriented towards measurable drought outcomes, (ii) comprehensive enough to capture key variables relevant for those outcomes and (iii) sensitive to species/phenotypic differences in those outcomes. The weaknesses of existing schemes for predicting drought responses can be attributed to their failure to meet one or more of these requirements. In particular, the difficulties in adopting trait-based or plant water potential-based metrics of drought vulnerability are related to their tendency to neglect or confound the role of the environment (Hochberg *et al.* 2018). We have shown here through sensitivity analysis that ecohydrological variables like vapour pressure deficit, dry season duration and rainfall have as much explanatory power for variation in drought outcomes for different species in some settings as physiological and morphological traits, as indicated by the strength of the Sobol' indices in Fig. 2. Without accounting explicitly for both the ecophysiological and ecohydrological contexts of drought stress, these metrics will potentially produce convergent results for different species in the same environment, or divergent results for the same species in different environments. This leads us to highlight the importance of considering not only the internal physiological pathways through which water stress may translate to plant stress and possibly death, but also their interactions with meteorological conditions (in their multiple axes of timing, duration and intensity; Feng *et al.* 2013), edaphic properties, topographical positions and other mitigating factors that together define a 'physiological drought' (Bhaskar *et al.* 2007; Anderegg *et al.* 2013a; Mitchell *et al.* 2013; McLaughlin *et al.* 2017).

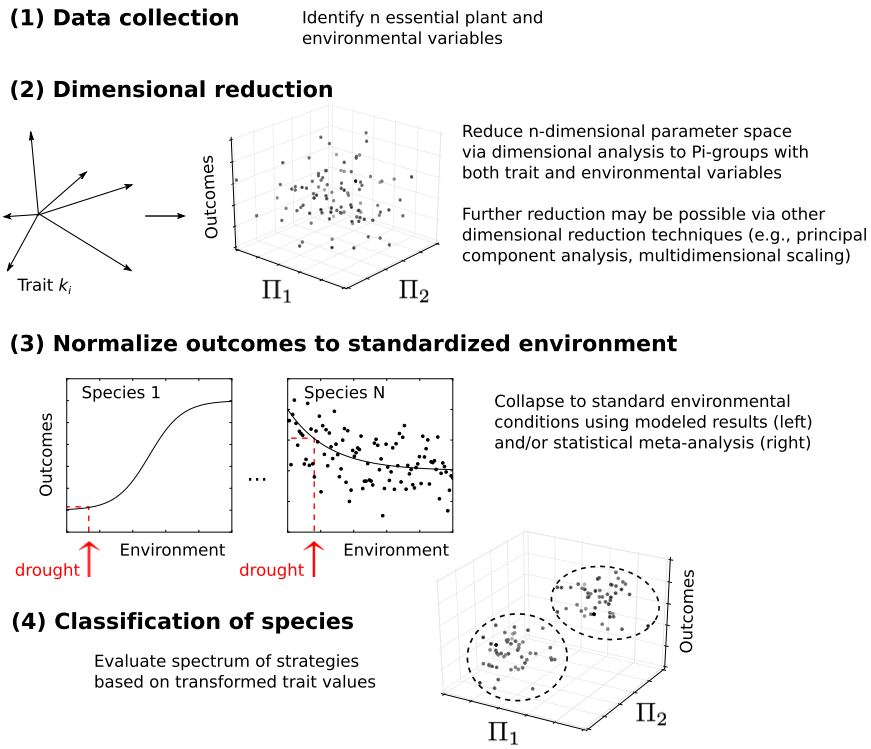

Figure 5 Schematic roadmap for a classification scheme for plant drought responses. Π indicates a generic non-dimensional parameter group.

In practice, the influence of environmental variation on the dimensionless groups (or any other axes of variation) potentially confounds direct comparison of drought outcomes between species observed in different environments. A productive line of inquiry could explore whether observations made under different environments could be converted to standardised drought risk estimates by normalising with respect to their local environments. This is consistent with the way the non-dimensional groups are defined, and can facilitate comparisons between plants that, for example, reside at the centre versus the edge of their natural range. Similar approaches could attempt to evaluate plants' drought risks in a common environment (analogous to the standard temperature and pressure reported by chemists). By controlling for environmental factors, this conversion could provide a basis for classifying plants based on trait contributions to drought vulnerability. Potentially, these drought risk estimates could be made by fitting plant hydraulic models like the one used in this study, or via meta-analysis of large trait databases across multiple environments (Fig. 5, step 3). Once these observations have been collapsed to a standardised environment, the spectrum of plant traits and strategies can be analysed along the transformed axes using clustering analysis (Fig. 5, step 4).

Limitations

This approach is currently limited by the extent of our empirical understanding of drought stress pathways. This model focuses on resolving the dynamic feedback between atmospheric moisture supply and demand, soil moisture infiltration and storage, and plant water uptake defined by a suite of plant functional traits. This emphasis on soil and plant hydraulics is bolstered by the fact that plant hydraulic dysfunction has been implicated in almost all cases of drought-induced mortality (Hartmann *et al.* 2013; Anderegg *et al.* 2015a; Mencuccini *et al.* 2015; Rowland *et al.* 2015; Adams *et al.* 2017). However, the model does not account for carbon storage and allocation, which could influence the mobilisation of plant carbon reserves, nor does it impose other limitations on assimilation based on light, nutrients, carbon sink strength, temperature or variability in respiratory demand. The model omits an explicit accounting of stored water within plant tissues, phenological changes (e.g. seasonal leaf gain and loss, Vico *et al.* (2017)), or access to deep belowground moisture sources (e.g. groundwater). Finally, including the negative effects of low leaf water potential on carboxylation efficiency (Lawlor & Tezara 2009), carbon transport in phloem (Jensen *et al.* 2016) and carbon costs of xylem repair (Sperry *et al.* 2017) could introduce additional coupling between water and carbon dynamics within the plant.

In addition, the generality of the classification groups could be improved with additional testing against data sets of mortality across larger populations, though community-level data sets describing the full suite of plant traits needed to parameterise this scheme for multiple species remain scarce. Because there is very limited information on the covariation of plant hydraulic traits within and across species, it is possible that the combination of traits generated for testing the classification scheme, though not behaviourally unrealistic based on criteria similar to those set out by Mencuccini *et al.* (2015), may not be representative of trait combinations found in nature. We attempted to address the coordination of functional traits in the synthetic

plants by limiting their variation to a reasonable range of measured values. Further testing using measured traits from a larger set of species can help resolve this issue.

CONCLUSIONS

We introduced a roadmap to a classification system for plant drought responses – posed in terms of both seasonal hydraulic risk and normalised seasonal carbon assimilation – that is sensitive to shifts in a suite of plant-related as well as environmental and meteorological variables. The classification system is first considered through a model-based approach using an explicit hydrodynamic linkage between these variables and drought responses. A set of non-dimensional groupings, representing independent axes of variation, are then developed that separate real and synthetic species along a continuum of drought outcomes. While formulating these axes of variation makes up only the first few steps of the process, it lays the groundwork for constructing a classification scheme. As new and improved data sets emerge, the classification scheme should be iteratively tested and refined to ultimately advance our understanding of how plant characteristics and their environments might interact to influence drought outcomes.

ACKNOWLEDGEMENTS

XF was partially supported by NOAA Climate and Global Change Postdoctoral Fellowship. SM was supported by the Swedish Research Council Formas (2016–00998) and thanks the NIMBioS working group 'A DEB Model for Trees' for discussions on tree hydraulics. GV acknowledges the support by Swedish Research Council Formas (942-2016-1) and the project 'TC4F—Trees and Crops for the Future' funded through the Swedish government's Strategic Research Environment 'Sustainable use of Natural Resources'. The authors also acknowledge support from National Science Foundation IOS-1441396 and IOS-1457400, and thank Dr. William Anderegg and two anonymous reviewers for providing valuable suggestions towards improving the manuscript.

AUTHORSHIP

XF and SET designed the study. Discussions among all authors contributed to its subsequent conceptual and theoretical development. XF performed the modelling work and wrote the first draft of the manuscript, to which all authors contributed revisions.

DATA ACCESSIBILITY STATEMENT

The data used to parameterise the model have been clearly cited within the text and are publicly available. Model codes are available at https://github.com/feng-ecohydro/soil-plant-model.

REFERENCES

Adams, H.D., Luce, C.H., Breshears, D.D., Allen, C.D., Weiler, M., Hale, V.C. *et al.* (2012). Ecohydrological consequences of drought- and infestation-triggered tree die-off: insights and hypotheses. *Ecohydrology*, 5, 145–159.

Adams, H.D., Germino, M.J., Breshears, D.D., Barron-Gafford, G.A., Guardiola-Claramonte, M., Zou, C.B. *et al.* (2013). Nonstructural leaf carbohydrate dynamics of *Pinus edulis* during drought-induced tree mortality reveal role for carbon metabolism in mortality mechanism. *New Phytol.*, 197, 1142–1151.

Adams, H.D., Zeppel, M.J.B., Anderegg, W.R.L., Hartmann, H., Landhäusser, S.M., Tissue, D.T. *et al.* (2017). A multi-species synthesis of physiological mechanisms in drought-induced tree mortality. *Nat. Ecol. Evol.*, 1, 1285–1291.

Allen, C.D. (2010). A global overview of drought and heat-induced tree mortality reveals emerging climate change risks for forests. *For. Ecol. Manag.*, 259, 660–684.

Anderegg, W.R.L. (2015). Spatial and temporal variation in plant hydraulic traits and their relevance for climate change impacts on vegetation. *New Phytol.*, 205, 1008–1014.

Anderegg, L.D.L., Anderegg, W.R.L. & Berry, J.A. (2013a). Not all droughts are created equal: translating meteorological drought into woody plant mortality. *Tree Physiol.*, 33, 672–683.

Anderegg, W.R.L., Kane, J.M. & Anderegg, L.D.L. (2013b). Consequences of widespread tree mortality triggered by drought and temperature stress. *Nat. Clim. Chang.*, 3, 30–36.

Anderegg, W.R.L., Flint, A., Huang, C.-Y., Flint, L., Berry, J.A., Davis, F.W. *et al.* (2015a). Tree mortality predicted from drought-induced vascular damage. *Nat. Geosci.*, 8, 367–371.

Anderegg, W.R.L., Hicke, J.A., Fisher, R.A., Allen, C.D., Aukema, J., Bentz, B. *et al.* (2015b). Tree mortality from drought, insects, and their interactions in a changing climate Research review Tree mortality from drought, insects, and their interactions in a. *New Phytol.*, 208, 674–683.

Anderegg, W.R.L., Klein, T., Bartlett, M., Sack, L., Pellegrini, A.F.A. & Choat, B. (2016). Meta-analysis reveals that hydraulic traits explain cross-species patterns of drought-induced tree mortality across the globe. *Proc. Natl Acad. Sci.*, 113, 2–7.

Barenblatt, G.I. (1996). *Scaling, self-similarity, and intermediate asymptotics: dimensional analysis and intermediate asymptotics*. Cambridge University Press, Cambridge.

Bartlett, M.K., Klein, T., Jansen, S., Choat, B. & Sack, L. (2016). The correlations and sequence of plant stomatal, hydraulic, and wilting responses to drought. *Proc. Natl Acad. Sci.*, 113, 13098–13103.

Bennett, A.C., Allen, C.D., Anderson-teixeira, K.J., Bennett, A.C., Mcdowell, N.G., Allen, C.D. *et al.* (2015). Larger trees suffer most during drought in forests worldwide. *Nature Plants*, 1, 15139.

Bhaskar, R., Valiente-banuet, A. & Ackerly, D.D. (2007). Evolution of hydraulic traits in closely related species pairs from mediterranean and nonmediterranean environments of North America. *New Phytol.*, 176, 718–726.

Buckingham, E. (1914). *On physically similar systems: illustrations of the use of dimensional equations*. Phys. Rev, IV, pp. 354–376.

Bugmann, H. (1996). Functional types of trees in temperate and boreal forests : classification and testing. *J. Veg. Sci.*, 7, 359–370.

Budyko, M.I. (1974). *Climate and Life*. Academic Press, New York, NY.

Clapp, R.B. & Hornberger, G.M. (1978). Empirical equations for some soil hydraulic properties. *Water Resour. Res.*, 14, 601–604.

Cowan, I.R. (1982). Regulation of Water Use in Relation to Carbon Gain in Higher Plants. In *Physiological Plant Ecology II*. (eds Lange, O.E., Nobel, P.S., Osmond, C.B., Ziegler, H.). Springer-Verlag, Berlin, pp. 589–613.

Cowan, I.R. & Farquhar, G.D. (1977). Stomatal function in relation to leaf metabolism and environment. *Symp. Soc. Exp. Biol.*, 31, 471–505.

Curtis, W.D., Logan, J.D. & Parker, W.A. (1982). Dimensional analysis and the pi theorem. *Linear Algebra Appl.*, 47, 117–126.

Daly, E., Porporato, A. & Rodríguez-Iturbe, I. (2004). Coupled dynamics of photosynthesis, transpiration, and soil water balance. Part I: upscaling from hourly to daily level. *J. Hydrometeorol.*, 5, 546–558.

Dewar, R.C. (2002). The ball-berry-leuning and tardieu-davies stomatal models: synthesis and extension within a spatially aggregated picture of guard cell function. *Plant, Cell Environ.*, 25, 1383–1398.

Diffenbaugh, N.S., Swain, D.L. & Touma, D. (2015). Anthropogenic warming has increased drought risk in California. *Proc. Natl Acad. Sci.*, 112, 3931–3936.

Farquhar, G.D., von Caemmerer, S. & Berry, J.A. (1980). A biochemical model of photosynthetic CO_2 assimilation in leaves of C3 species. *Planta*, 149, 78–90.

Feng, X., Vico, G. & Porporato, A. (2012). On the effects of seasonality on soil water balance and plant growth. *Water Resour. Res.*, 48, W05543. https://doi.org/10.1029/2011WR011263.

Feng, X., Porporato, A. & Rodriguez-Iturbe, I. (2013). Changes in rainfall seasonality in the tropics. *Nat. Clim. Chang.*, 3, 811–815.

Feng, X., Dawson, T.E., Ackerly, D.D., Santiago, L.S. & Thompson, S.E. (2017). Reconciling seasonal hydraulic risk and plant water use through probabilistic soil-plant dynamics. *Glob. Chang. Biol.*, 23, 3758–69.

Givnish, T. (1988). Adaptation to sun and shade: a whole-plant perspective. *Aust. J. Plant Physiol.*, 15, 63–92.

Hari, P., Mäkelä, A., Korpilahti, E. & Holmberg, M. (1986). Optimal control of gas exchange. *Tree Physiology*, 2, 169–175.

Hartmann, H. & Trumbore, S. (2016). Understanding the roles of nonstructural carbohydrates in forest trees – from what we can measure to what we want to know. *New Phytol.*, 211, 386–403.

Hartmann, H., Ziegler, W., Kolle, O. & Trumbore, S. (2013). Thirst beats hunger - declining hydration during drought prevents carbon starvation in Norway spruce saplings. *New Phytol.*, 200, 340–349.

Hochberg, U., Rockwell, F.E., Holbrook, N.M. & Cochard, H. (2018). Iso/Anisohydry: a plant-environment interaction rather than a simple hydraulic trait. *Trends Plant Sci.*, 23, 112–120.

Jensen, K.H., Berg-Sørensen, K., Bruus, H., Holbrook, N.M., Liesche, J., Schulz, A. *et al.* (2016). Sap flow and sugar transport in plants. *Rev. Mod. Phys.*, 88, 035007.

Kattge, J., Díaz, S., Lavorel, S., Prentice, I.C., Leadley, P., Bönisch, G. *et al.* (2011). TRY - a global database of plant traits. *Glob. Chang. Biol.*, 17, 2905–2935.

Laio, F., Porporato, A., Ridol, L. & Rodriguez-Iturbe, I. (2001). Plants in water-controlled ecosystems: active role in hydrologic processes and response to water stress II. Probabilistic soil moisture dynamics. *Adv. Water Resour.*, 24, 707–723.

Lawlor, D.W. & Tezara, W. (2009). Causes of decreased photosynthetic rate and metabolic capacity in water-deficient leaf cells: a critical evaluation of mechanisms and integration of processes. *Ann. Bot.*, 103, 561–579.

Manzoni, S., Vico, G., Katul, G., Palmroth, S. & Porporato, A. (2014). Optimal plant water-use strategies under stochastic rainfall. *Water Resour. Res.*, 50, 5379–5394.

Martin-StPaul, N., Delzon, S., Cochard, H. & Maherali, H. (2017). Plant resistance to drought depends on timely stomatal closure. *Ecol. Lett.*, 20, 1437–1447. https://doi.org/10.1111/ele.12851.

Martínez-Vilalta, J. & Garcia-Forner, N. (2016). Water potential regulation, stomatal behaviour and hydraulic transport under drought: deconstructing the iso/anisohydric concept. *Plant, Cell Environ.*, 8193, 1–15.

Martínez-Vilalta, J., Piñol, J. & Beven, K. (2002). A hydraulic model to predict drought-induced mortality in woody plants: an application to climate change in the Mediterranean. *Ecol. Modell.*, 155, 127–147.

Matheny, A.M., Mirfenderesgi, G. & Bohrer, G. (2017). Plant diversity trait-based representation of hydrological functional properties of plants in weather and ecosystem models. *Plant Divers.*, 39, 1–12.

McCulloh, K.A. & Meinzer, F.C. (2015). Further evidence that some plants can lose and regain hydraulic function daily. *Tree Physiol.*, 35, 691–693.

McCulloh, K.A., Johnson, D.M., Meinzer, F.C. & Woodruff, D.R. (2014). The dynamic pipeline: hydraulic capacitance and xylem hydraulic safety in four tall conifer species. *Plant, Cell Environ.*, 37, 1171–1183.

McDowell, N.G. (2011). Mechanisms linking drought, hydraulics, carbon metabolism, and vegetation mortality. *Plant Physiol.*, 155, 1051–9.

McDowell, N., Pockman, W.T., Allen, C.D., David, D., Cobb, N., Kolb, T. *et al.* (2008). Mechanisms of plant survival and mortality during drought: why do some plants survive while others succumb to drought? *New Phytol.*, 178, 719–739.

McDowell, N.G., Beerling, D.J., Breshears, D.D., Fisher, R.A., Raffa, K.F. & Stitt, M. (2011). The interdependence of mechanisms underlying climate-driven vegetation mortality. *Trends Ecol. Evol.*, 26, 523–32.

McDowell, N.G., Fisher, R.A., Xu, C., Domec, J.C., Hölttä, T., Mackay, D.S. *et al.* (2013a). Evaluating theories of drought-induced vegetation mortality using a multimodel-experiment framework. *New Phytol.*, 200, 304–321.

McDowell, N.G., Ryan, M.C., Zeppel, M.J.B. & Tissue, D.T. (2013b). Improving our knowledge of drought-induced forest mortality through experiments, observations, and modeling. *New Phytol.*, 200, 289–293.

McLaughlin, B.C., Ackerly, D.D., Klos, P.Z., Natali, J., Dawson, T.E. & Thompson, S.E. (2017). Hydrologic refugia, plants, and climate change. *Glob. Chang. Biol.*, 23, 2941–61.

Meinzer, F.C., Johnson, D.M., Lachenbruch, B., Mcculloh, K.A. & Woodruff, D.R. (2009). Xylem hydraulic safety margins in woody plants: coordination of stomatal control of xylem tension with hydraulic capacitance. *Funcitional Ecol.*, 23, 922–930.

Mencuccini, M., Minunno, F., Salmon, Y., Martínez-Vilalta, J. & Hölttä, T. (2015). Coordination of physiological traits involved in drought-induced mortality of woody plants. *New Phytol.*, 208, 396–409.

Mitchell, P.J., O'Grady, A.P., Tissue, D.T., White, D.A., Ottenschlaeger, M.L. & Pinkard, E.A. (2013). Drought response strategies define the relative contributions of hydraulic dysfunction and carbohydrate depletion during tree mortality. *New Phytol.*, 197, 862–872.

Noble, I.R. & Gitay, H. (1996). A functional classification for predicting the dynamics of landscapes. *J. Veg. Sci.*, 7, 329–336.

O'Brien, M.J., Leuzinger, S., Philipson, C.D., Tay, J., Hector, A., Brien, M.J.O. *et al.* (2014). Drought survival of tropical tree seedlings enhanced by non-structural carbohydrate levels. *Nat. Clim. Chang.*, 4, 710–714.

O'Brien, M.J., Engelbrecht, B.M., Joswig, J., Pereyra, G., Schuldt, B., Jansen, S. *et al.* (2017). A synthesis of tree functional traits related to drought-induced mortality in forests across climatic zones. *J. Appl. Ecol.*, 54, 1669–1686.

Pammenter, N.W. & Willigen, C.V. (1998). A mathematical and statistical analysis of the curves illustrating vulnerability of xylem to cavitation. *Tree Physiol.*, 18, 589–593.

Park Williams, A., Allen, C.D., Macalady, A.K., Griffin, D., Woodhouse, C.A., Meko, D.M. *et al.* (2012). Temperature as a potent driver of regional forest drought stress and tree mortality. *Nat. Clim. Chang.*, 3, 292–297.

Parolari, A.J., Katul, G.G. & Porporato, A. (2014). An ecohydrological perspective on drought-induced forest mortality. *J. Geophys. Res. Biogeosciences*, 119, 965–981.

Phillips, O.L., Aragão, L.E.O.C., Lewis, S.L., Fisher, J.B., Lloyd, J., López-González, G. *et al.* (2009). Drought sensitivity of the Amazon rainforest. *Science*, 323, 1344–1347.

Pianka, E.R. (1970). On r- and K-selection. *Am. Nat.*, 107, 592–597.

Pivovaroff, A.L., Pasquini, S.C., De Guzman, M.E., Alstad, K.P., Stemke, J.S., Santiago, L.S. *et al.* (2016). Multiple strategies for drought survival among woody plant species. *Funcitional Ecol.*, 30, 517–526.

Porporato, A., Daly, E. & Rodriguez-iturbe, I. (2004). Soil water balance and ecosystem response to climate change. *Am. Nat.*, 164, 625–632.

Powell, T.L., Galbraith, D.R., Christoffersen, B.O., Harper, A., Imbuzeiro, H.M.A., Rowland, L. *et al.* (2013). Confronting model predictions of carbon fluxes with measurements of Amazon forests subjected to experimental drought. *New Phytol.*, 200, 350–364.

Rodriguez-Iturbe, I. & Porporato, A. (2004). *Ecohydrology of Water-Controlled Ecosystems*. Cambridge University Press, Cambridge, UK.

Ross, P.J. & Bristow, K.L. (1990). Simulating water movement in layered and gradational soils using the kirchhoff transform. *Soil Sci. Soc. Am. J.*, 54, 1519.

Rowland, L., da Costa, A.C.L., Galbraith, D.R., Oliveira, R.S., Binks, O.J., Oliveira, A.A.R. *et al.* (2015). Death from drought in tropical

forests is triggered by hydraulics not carbon starvation. *Nature*, 528, 119–122.
Settele, J., Scholes, R., Betts, R.A., Bunn, S., Leadley, P., Nepstad, D. *et al.* (2015b). Terrestrial and Inland water systems. In: *Climate Change 2014 Impacts, Adaptation and Vulnerability: Part A: Global and Sectoral Aspects* (pp. 271–360). Cambridge University Press. DOI: 10.1017/CBO9781107415379.009
Sevanto, S., Mcdowell, N.G., Dickman, L.T., Pangle, R. & Pockman, W.T. (2014). How do trees die? A test of the hydraulic failure and carbon starvation hypotheses. *Plant, Cell Environ.*, 37, 153–161.
Siefert, A., Violle, C., Chalmandrier, L., Albert, C.H., Taudiere, A., Fajardo, A. *et al.* (2015). A global meta-analysis of the relative extent of intraspecific trait variation in plant communities. *Ecol. Lett.*, 18, 1406–1419.
Sitch, S., Huntingford, C., Gedney, N., Levy, P.E., Lomas, M., Piao, S.L. *et al.* (2008). Evaluation of the terrestrial carbon cycle, future plant geography and climate-carbon cycle feedbacks using five Dynamic Global Vegetation Models (DGVMs). *Glob. Chang. Biol.*, 14, 2015–2039.
Skelton, R.P., West, A.G. & Dawson, T.E. (2015). Predicting plant vulnerability to drought in biodiverse regions using functional traits. *Proc. Natl Acad. Sci.*, 112, 5744–5749.
Skelton, R.P., Brodribb, T.J., Mcadam, S.A.M. & Mitchell, P.J. (2017). Gas exchange recovery following natural drought is rapid unless limited by loss of leaf hydraulic conductance: evidence from an evergreen woodland. *New Phytol.*, 215, 1399–412.
Skelton, R.P., Dawson, T.E., Thompson, S.E., Shen, Y., Weitz, A.P. & Ackerly, D. (2018). Low vulnerability to xylem embolism in leaves and stems of North American oaks. *Plant Physiol.*, May 2018, pp.00103.2018; DOI: 10.1104/pp.18.00103
Sobol', I.M. (2001). Global sensitivity indices for nonlinear mathematical models and their Monte Carlo estimates. *Math. Comput. Simul.*, 55, 271–280.
Sperry, J.S. & Love, D.M. (2015). What plant hydraulics can tell us about responses to climate-change droughts. *New Phytol.*, 207, 14–27.
Sperry, J.S., Adler, F.R., Campbell, G.S. & Comstock, J.P.C.N. (1998). Limitation of plant water use by rizosphere and xylem conductance: results of a model. *Plant, Cell Environ.*, 21, 347–359.
Sperry, J.S., Wang, Y., Wolfe, B.T., Mackay, D.S., Anderegg, W.R.L., McDowell, N.G. *et al.* (2016). Pragmatic hydraulic theory predicts stomatal responses to climatic water deficits. *New Phytol.*, 212, 577–589.
Sperry, J.S., Venturas, M.D., Anderegg, W.R.L., Mencuccini, M., Mackay, D.S., Wang, Y. *et al.* (2017). Predicting stomatal responses to the environment from the optimization of photosynthetic gain and hydraulic cost. *Plant, Cell Environ.*, 40, 816–830.
Strogatz, S.H. (1994). *Nonlinear dynamics and chaos: with applications to physics, biology, chemistry, and engineering*. Westview Press, Boulder, CO.
Sutera, S.P. & Skalak, R. (1993). The history of Poiseuille law. *Annu. Rev. Fluid Mech.*, 25, 1.
Swann, A.L.S., Longo, M., Knox, R.G., Lee, E. & Moorcroft, P.R. (2015). Future deforestation in the Amazon and consequences for South American climate. *Agric. For. Meteorol.*, 214–215, 12–24.
Symstad, A.J. (2002). An overview of ecological plant classification systems. In: *Modern Trends in Applied Terrestrial Ecology*. Springer, Boston, MA, pp. 13–50.
Tardieu, F., Simonneau, T. & Simmonneau, T. (1998). Variability among species of stomatal control under fluctuating soil water status and evaporative demand: modelling isohydric and anisohydric behaviours. *J. Exp. Bot.*, 49, 419–432.
Trifilo, P., Nardini, A., Gullo, M.A.Lo, Barbera, P.M., Savi, T. & Raimondo, F. (2015). Diurnal changes in embolism rate in nine dry forest trees: relationships with species-specific xylem vulnerability, hydraulic strategy and wood traits. *Tree Physiol.*, 35, 694–705.
Urli, M., Porté, A.J., Cochard, H., Guengant, Y., Burlett, R. & Delzon, S. (2013). Xylem embolism threshold for catastrophic hydraulic failure in angiosperm trees. *Tree Physiol.*, 33, 672–683.
van der Molen, M.K., Dolman, A.J., Ciais, P., Eglin, T., Gobron, N., Law, B.E. *et al.* (2011). Drought and ecosystem carbon cycling. *Agric. For. Meteorol.*, 151, 765–773.
Van Bodegom, P.M., Douma, J.C., Witte, J.P.M., Ordoñez, J.C., Bartholomeus, R.P. & Aerts, R. (2012). Going beyond limitations of plant functional types when predicting global ecosystem-atmosphere fluxes: exploring the merits of traits-based approaches. *Glob. Ecol. Biogeogr.*, 21, 625–636.
Van den Bilcke, N., De Smedt, S., Simbo, D.J. & Samson, R. (2013). Sap flow and water use in African baobab (*Adansonia digitata* L.) seedlings in response to drought stress. *South African J. Bot.*, 88, 438–446.
Verhulst, P.-F. (1838). Notice sur la loi que la population suit dans son accroissement. correspondance mathématique et physique publiée par a. *Quetelet*, 10, 131–121.
Vico, G., Dralle, D., Feng, X., Thompson, S. & Manzoni, S. (2017). How competitive is drought deciduousness in tropical forests? A combined eco-hydrological and eco-evolutionary approach. *Environ. Res. Lett.*, 12, 65006.
Whitehead, D., Edwards, W.R.N. & Jarvis, P.G. (1984). Conducting sapwood area, foliage area, and permeability in mature trees of *Picea sitchensis* and *Pinus contorta*. *Can. J. For. Res.*, 14, 940–947.
Winkler, R.D., Moore, R.D., Redding, T.E., Spittlehouse, D.L., Smerdon, B.D. & Carlyle-Moses, D.E. (2010). The effects of forest disturbance on hydrologic processes and watershed. *Compend. For. Hydrol. Geomorphol. Br. Columbia. BC Min. For. Range*, 66, 179.
Wright, J.P., Naeem, S., Hector, A., Lehman, C., Reich, P.B., Schmid, B. *et al.* (2006). Conventional functional classification schemes underestimate the relationship with ecosystem functioning. *Ecol. Lett.*, 9, 111–120.
Wullschleger, S.D., Epstein, H.E., Box, E.O., Euskirchen, E.S., Goswami, S., Iversen, C.M. *et al.* (2014). Plant functional types in Earth system models: past experiences and future directions for application of dynamic vegetation models in high-latitude ecosystems. *Ann. Bot.*, 114, 1–16.

SUPPORTING INFORMATION

Additional supporting information may be found online in the Supporting Information section at the end of the article.

Editor, Hafiz Maherali
Manuscript received 8 March 2018
First decision made 12 April 2018
Second decision made 7 July 2018
Manuscript accepted 16 July 2018